RARE METALS
Vol. 29, No. 4, Aug 2010, p. 385
DOI: 10.1007/s12598-010-0135-y

Fabrication and magnetic properties of $NiFe_2O_4$ nanorods

WU Yue[a, b], SHI Changhong[c], and YANG Wei[a]

[a] *National Key Laboratory for Electronic Measurement Technology, North University of China, Taiyuan 030051, China*
[b] *School of Mechanical and Electronic Engineering, North University of China, Taiyuan 030051, China*
[c] *The Quartermaster Institute of the General Logistics Department of the PLA, Beijing 100010, China*

Received 15 August 2009; received in revised form 15 March 2010; accepted 20 March 2010

Abstract

$NiFe_2O_4$ nanorods have been successfully synthesized via thermal treatment of the rod-like precursor fabricated by Ni-doped α-FeOOH, which was enwrapped by the complex of citric acid and Ni^{2+}. The morphology evolution during the calcination of the precursor nanorods was investigated with transmission electron microscopy (TEM), and the phase and the magnetic properties of samples were analyzed through X-ray diffraction (XRD) and vibrating sample magnetometer (VSM). The results indicated that the diameter of the $NiFe_2O_4$ nanorods obtained ranged between 30 and 50 nm, and the length ranged between 2 and 3 μm. As the calcination temperature was up to 600°C, the coercivity, saturation magnetization, and remanent magnetization of the samples were 36.1 $kA \cdot m^{-1}$, 27.2 $A \cdot m^2 \cdot kg^{-1}$, and 5.3 $A \cdot m^2 \cdot kg^{-1}$, respectively. The $NiFe_2O_4$ nanorods prepared have higher shape anisotropy and superior magnetic properties than those with irregular shapes.

Keywords: inorganic compounds; nickel ferrite; nanorods; electron microscopy; magnetic properties

1. Introduction

As an important magnetic material, ferrite has been widely used in a variety of technological fields like biology, electronics, transport, and information technology [1-4] for high-density data storage [5], ferrofluids making [6], magnetic resonance imaging (as contrast agents), and magnetic refrigeration [7]. As against ferro-spinel magnetic material, one-dimensional nanostructural magnetic material is particularly interesting to researchers due to its high magneto crystalline anisotropy, high saturation magnetization, and unique magnetic structure [8]. Nickel ferrite ($NiFe_2O_4$), originating from magnetic moment of antiparallel spins between Fe^{3+} ions at tetrahedral sites and Ni^{2+} ions at octahedral sites with an inverse spinel structure, for example, shows ferrimagnetism [9] with unique and amazing properties compared to its bulk counterpart. Based on a bottom-up paradigm, magnetic material with one-dimensional nanostructure can be used to fabricate functional nanoscale electronic, optoelectronic, photonic, chemical, and biomedical devices [10-12]. Many researches have been made on the synthesis of one-dimensional nanostructures nickel ferrite. The properties of synthesized magnetic material are dependent on its composition and microstructure; they are also sensitive to its preparation methods. Many methods have been so far proposed for the preparation of nanocrystallite $NiFe_2O_4$, including sol-gel method [13], coprecipitation method [14], hydrothermal method [15], combustion method [16], mechanochemical method [17], precursor method [18], and microemulsion method [19], etc. Since the behaviors of nanophase magnetic material depend strongly on the shape and size of the magnetic material particles, control of the shape and size of the particles is the key factor determining their ultimate performance and applications.

In this paper, $NiFe_2O_4$ nanorods with the aspect ratio higher than 20 have been synthesized through thermal treatment of the rod-like precursor, and the magnetic properties of the $NiFe_2O_4$ nanoparticles prepared were investigated. The rod-like precursor has been obtained from Ni-doped α-FeOOH enwrapped by citric acid and Ni^{2+} solution. The morphologically controlled transformation of amorphous precursor nanorods into crystalline nanorods is remarkably similar to the petrification process that happens in nature with a timescale of several centuries [20].

2. Experimental

All the reagents were of analytical grade and were used as received without further purification. Nickel nitrate [$Ni(NO_3)_2 \cdot 6H_2O$], ferrous chloride [$Fe(Cl)_2 \cdot 4H_2O$], and so-

Corresponding author: WU Yue **E-mail:** wuy@live.nuc.edu.cn

dium hydroxide [NaOH] were purchased from Shanxi Chemical Reagent Co.

$FeCl_2$ and $Ni(NO_3)_2$ (the optimum mole ratio of $n(Ni^{2+}):n(Fe^{2+})$ is 1:20 [21]) were dissolved in deionized water. According to $m(NaOH)/m(FeCl_2)$ of 1.0:3.5 (mass ratio), NaOH was dissolved in another deionized water to prepare alkali liquor. Then, the alkali liquor was poured into $FeCl_2$ and $Ni(NO_3)_2$ solution. The above mixture was stirred in magnetic blender at 50°C for 12 h. The product was then filtered and washed several times until its pH value reached 7. The precipitate was dried in a cabinet dryer at 80°C for 12 h to obtain Ni-doped α-FeOOH nanorods samples.

The self-made Ni-doped α-FeOOH nanorods were poured into deionized water and were dispersed in ultrasonic wave atmosphere to obtain Ni-doped α-FeOOH suspension. $Ni(NO_3)_2$ weighted according to $n(Ni^{2+}):n(Fe^{2+})$ of 9:20 (mole ratio) was dissolved in another deionized water. Then, based on the mole ratio of citric acid:Ni^{2+} of 1:1, citric acid was added to the $Ni(NO_3)_2$ solution, and $NH_3{\cdot}H_2O$ was used to adjust the pH value to 6 after the solution being agitated homogeneously. Subsequently, the solution was heated and agitated until its volume was approximately 10 mL to form sol. The suspension was dipped into the sol and was agitated to form gel on the surface of Ni-doped α-FeOOH. Then, the gel was dried in a cabinet dryer at 90°C to obtain precursor samples. The precursor samples were calcined for 3 h at the temperatures of 500, 600, and 700°C, respectively, to obtain $NiFe_2O_4$ samples.

The synthesized $NiFe_2O_4$ samples were subsequently characterized by X-ray diffraction (XRD, Rigaku D/max-gB X-ray diffractometer with Cu K_α radiation) and transmission electron microscope (TEM). The magnetic properties of $NiFe_2O_4$ samples were measured using a vibrating sample magnetometer (VSM) at room temperature under a maximum field of 800 $kA{\cdot}m^{-1}$.

3. Results and discussion

Phase identification of the as-prepared sample was examined by XRD. Fig. 1(a) shows the XRD pattern of the precursor. These peaks were indexed to the α-FeOOH phase according to the JCPDS (Card No. 24-1207) standard, showing that, in the precursor, the Ni^{2+} took up the position of Fe^{3+} in the α-FeOOH crystal lattice, rather than existing in the form of $Ni(OH)_2$. Figs. 1(b-d) show XRD patterns of the as-synthesized $NiFe_2O_4$ nanorods obtained after annealing at different temperatures (500, 600, and 700°C) for 3 h in air. According to Fig. 1, some α-Fe_2O_3 appeared in the samples at the temperature lower than 600°C. As the calcination temperature was up to 600°C, all of the detectable peaks can be readily indexed as $NiFe_2O_4$ with an inverse spinel structure, as shown in the standard data (JCPDS Card No. 10-0325), and no characteristic peaks of impurities were detected. As the annealing temperature increased, the reflection peaks became sharper and narrower, indicating the improvement of crystallinity.

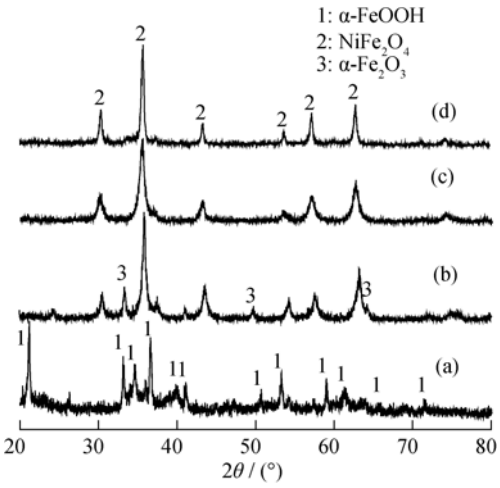

Fig. 1. XRD patterns of Ni-doped α-FeOOH and as-prepared $NiFe_2O_4$ samples: (a) precursor; (b) annealed at 500°C; (c) annealed at 600°C; (d) annealed at 700°C.

The morphology and particle size of the as-prepared samples and the precursor were characterized by TEM. Fig. 2 shows the TEM images of the precursor and $NiFe_2O_4$ samples. As Fig. 2(a) shows, a rod-like morphology with an average diameter of 40 nm and an average length of 3 μm was observed. The surface of amorphous precursor rods was very smooth. Figs. 2(b-d) are the TEM images of the $NiFe_2O_4$ samples annealed at 500, 600, and 700°C, respectively. It can be seen from the images that the overall dimensions of rods have not changed, with their diameter in the range of 30-50 nm and their length in the range of 2-3 μm. Compared with the morphology of the precursor, the diameter of the rod-like $NiFe_2O_4$ increased, and the length reduced appreciably as the temperature increased. Some aggregations appeared in the samples as the calcination temperature reached up to 700°C.

According to Ref. [22], in the preparation of α-FeOOH nanorods via chemical precipitation-air oxidation method, $Fe(OH)_2$ and $Ni(OH)_2$ formed first in the lye. $Ni(OH)_2$ was dissolvable, and the following dissolution equation existed in the solution:

$$Ni(OH)_2 \leftrightarrow Ni^{2+} + 2OH^-.$$

As time went on, $Fe(OH)_2$ was oxidized to form α-FeOOH in the air atmosphere. In the process, the crystal growth of acicular α-FeOOH was anisomerous; the growth rate was the fastest in the direction of the strongest bond. The Ni^{2+} having the similar radius and Fe^{3+} charge entered

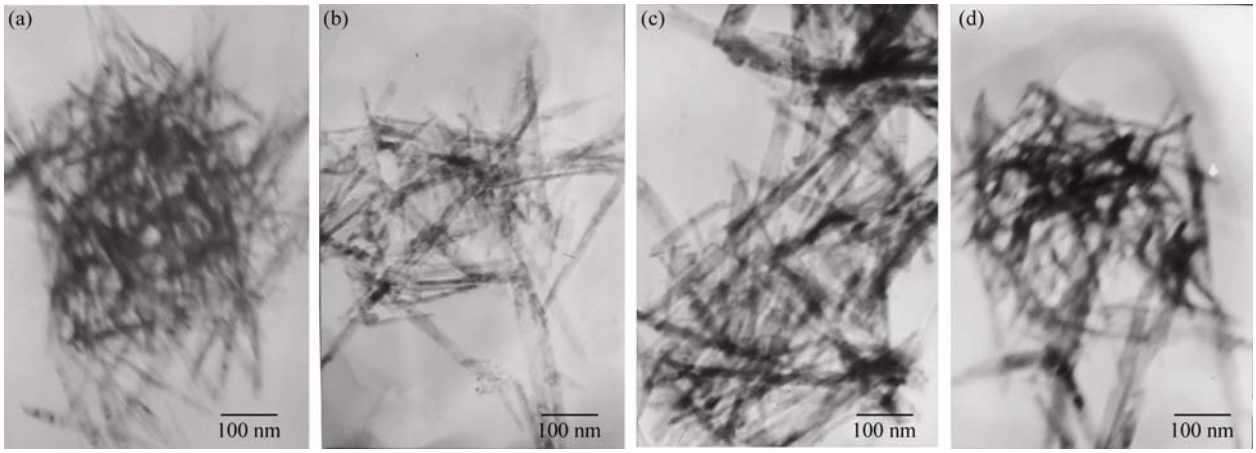

Fig. 2. TEM photographs of Ni-doped α-FeOOH and as-prepared $NiFe_2O_4$ samples: (a) precursor; (b) annealed at 500°C; (c) annealed at 600°C; (d) annealed at 700°C.

the inside of the crystal and held the position of the Fe^{3+} in the direction of the strongest bond, resulting in the decreasing of the energy which the crystalline growth needed to overcome and the increasing of the growth rate of α-FeOOH microlite in the direction of the strongest bond [23]. According to Ref. [21], the diameter of the α-FeOOH nanorod reduced in the above process, resulting in the increase in aspect ratio. The morphology of the precursor obtained by enwrapping the complex of citric acid and Ni^{2+} on the surface of α-FeOOH nanorods was the same as that of α-FeOOH. The nanorods kept their original morphology through the whole calcination process. The microstructural change was initiated by coalescence of the crystalline nanoparticles generated by the continuous decomposition of precursor at relatively high temperatures within the rods. Therefore, the crystalline nanorods were transformed from the amorphous precursor nanorods without destruction of the original morphology.

Magnetization measurement of the as-prepared sample was conducted using a vibrating sample magnetometer with a magnetic field up to 800 $kA \cdot m^{-1}$. Fig. 3 and Table 1 show the magnetic properties of $NiFe_2O_4$ obtained under different conditions, and show that the samples obtained at 500, 600, and 700°C have clear magnetic hysteresis loops, with coercivities of 29.9, 36.1, and 33.6 $kA \cdot m^{-1}$, respectively. There existed α-Fe_2O_3 phase in the sample obtained at 500°C and crystal defect in the sample obtained at 700°C. Thus, the coercivities of the samples first increased and then reduced as the temperature increased, and the coercivity reached the maximum at 600°C. The saturation magnetization increased as the temperature increased.

It has been reported that the particle size influences the magnetic properties of materials [24-25]. For monodomain particles, saturation magnetization decreases as the crystallite size decreases because of spin canting of magnetic domain on the microcrystallite surface and thermal fluctuation. Taking XRD and TEM results into consideration, the authors suggest that good crystallinity of the sample and more formation of magnetic phase due to higher temperature aroused the significant increase in saturation magnetization.

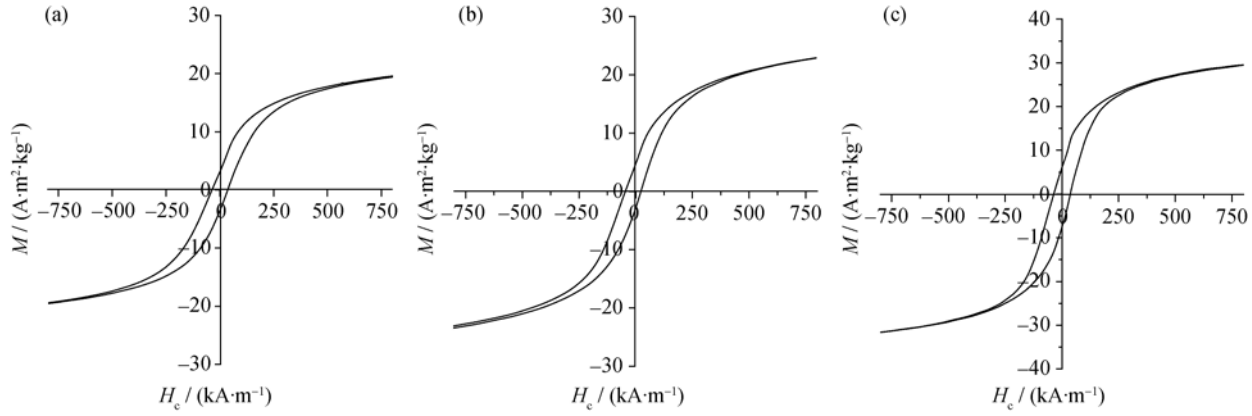

Fig. 3. Magnetic hysteresis loops of the as-prepared $NiFe_2O_4$ samples annealed at different temperatures: (a) 500°C; (b) 600°C; (c) 700°C.

Table 1. Magnetization measurement of as-prepared $NiFe_2O_4$ samples

Temperature, T / °C	Coercivity, H_c / (kA·m^{-1})	Remanent magnetization, M_r / (A·m^2·kg^{-1})	Saturation magnetization, M_s / (A·m^2·kg^{-1})
500	29.9	4.5	22.9
600	36.1	5.3	27.2
700	33.6	5.7	34.1

It was earlier reported in Ref. [19] that the nickel ferrite nanoparticles, with irregular shapes and sizes from 10 to 30 nm, exhibited lower coercivity (28.1 kA·m^{-1}) compared to the values (36.1 kA·m^{-1}) of our samples obtained after being annealed at 600°C. The difference in coercivity is mainly caused by the differences in particle morphology [26]. As the presence of shape anisotropy significantly enhances the magnetic properties [27], a higher aspect ratio facilitates the increase of coercivity.

4. Conclusion

$NiFe_2O_4$ nanorods have been successfully synthesized through thermal treatment of the rod-like precursor fabricated by Ni-doped α-FeOOH, which was enwrapped by the complex of citric acid and Ni^{2+}. The morphology evolution during calcination of the precursor nanorods was investigated by TEM. The phase and magnetic properties of $NiFe_2O_4$ samples were analyzed through X-ray diffraction (XRD) and vibrating sample magnetometer (VSM). It can be found that the diameters of $NiFe_2O_4$ nanorods obtained ranged between 30 and 50 nm, and the length ranged between 2 and 3 μm. As the calcination temperature increased, the length of rod-like $NiFe_2O_4$ reduced, and the diameter increased appreciably. As the calcination temperature was up to 600°C, the coercivity, saturation magnetization, and remanent magnetization of the sample were 36.1 kA·m^{-1}, 27.2 A·m^2·kg^{-1}, and 5.3 A·m^2·kg^{-1}, respectively.

Acknowledgements

The authors acknowledge the North University of China and the National Natural Science Foundation of China (No. 50535030) for financial support to this work.

References

[1] Ziolo R.F., Giannelis E.P., Weinstein B.A., O'Horo M.P., Ganguli B.N., Mehrotra V., Russel M.W., and Huffman D.R., Matrix-mediated synthesis of nanocrystalline γ-ferric oxide: A new optically transparent magnetic material, *Science*, 1992, **257**(5067): 219.

[2] Wirtz D. and Fermigier M., One-dimensional patterns and forced periodicity in magnetic fluids, *Phys. Rev. Lett.*, 1994, **72** (14): 2294.

[3] Masala O., Hoffman D., Sundaram N., Page K., Proffen T., Lawes G., and Seshadri R., Preparation of magnetic spinel ferrite core/shell nanoparticles: Soft ferrites on hard ferrites and vice versa, *Solid State Sci*., 2006, **8** (9): 1015.

[4] Cvejic Z., Rakic S., Kremenovic, A. Antic B., Jovaleki C., and Colomban P., Nanosize ferrites obtained by ball milling: Crystal structure, cation distribution, size-strain analysis and Raman investigations, *Solid State Sci*., 2006, **8** (8): 908.

[5] Speliotis D.E., Magnetic recording beyond the first 100 years, *J. Magn. Magn. Mater*., 1999, **193** (1-3): 29.

[6] Raj K., Moskowitz B., and Casciari R., Advances in ferrofluid technology, *J. Magn. Magn. Mater*., 1995, **149** (1-2): 174.

[7] Wang J., Zhua Y.J., Lia W.P., and Chen Q.W., Necklace-shaped assembly of single-crystal $NiFe_2O_4$ nanospheres under magnetic field, *Mater. Lett*., 2005, **59** (16): 2101.

[8] Cheng Y., Zheng Y.H., Wang Y.S., Bao F., and Qin Y., Synthesis and magnetic properties of nickel ferrite nano-octahedra, *J. Solid State Chem*., 2005, **178** (7): 2394.

[9] Kinemuchi Y., Ishizaka K., Suematsu H., Jiang W., and Yatsui K., Magnetic properties of nanosize $NiFe_2O_4$ particles synthesized by pulsed wire discharge, *Thin Solid Films*, 2002, **407** (1-2): 109.

[10] Huang Y., Duan X.F., Wei Q.Q., and Lieber C.M., Directed assembly of one-dimensional nanostructures into functional networks, *Science*, 2001, **291** (5504): 630.

[11] Gudiksen M.S., Lauhon L.J., Wang J., Smith D.C., and Lieber C.M., Growth of nanowire superlattice structures for nanoscale photonics and electronics, *Nature*, 2002, **415**: 617.

[12] Mieszawska A.J., Jalilian R., Sumanasekera G.U., and Zamborini F.P., The synthesis and fabrication of one-dimensional nanoscale heterojunctions, *Small*, 2007, **3** (5): 722.

[13] Chatterjee A., Das D., Pradhan S.K., and Chakravorty D., Synthesis of nanocrystalline nickel-zinc ferrite by the sol-gel method, *J. Magn. Magn. Mater*., 1993, **127** (1-2): 214.

[14] Doh S.G., Kim E.B., Lee B.H., and Oh J.H., Characteristics and synthesis of Cu-Ni ferrite nanopowders by coprecipitation method with ultrasound irradiation, *J. Magn. Magn. Mater*., 2004, **272-276** (3): 2238.

[15] Baruwati B., Rana R.K., and Manorama S.V., Further insights in the conductivity behavior of nanocrystalline $NiFe_2O_4$, *J. Appl. Phys*., 2007, **10**: 014302.

[16] Balaji S., Selvan R.K., Berchmans L.J., Angappan S., Subramanian K., and Augustin C.O., Combustion synthesis and characterization of Sn^{4+} substituted nanocrystalline $NiFe_2O_4$, *Mater. Sci. Eng. B*, 2005, **119** (2): 119.

[17] Yang H.M., Zhang X.C., Ao W.Q., and Qiu G.Z., Formation

of $NiFe_2O_4$ nanoparticles by mechanochemical reaction, *Mater. Res. Bull*., 2004, **39** (6): 833.

[18] Li X.D., Yang W.S., Li F., Evans D.G., and Duan X., Stoichiometric synthesis of pure $NiFe_2O_4$ spinel from layered double hydroxide precursors for use as the anode material in lithium-ion batteries, *J. Phys. Chem. Solids*, 2006, **67** (5-6): 1286.

[19] Jiang J., Yang Y.M., and Li L.C., Surfactant-assisted synthesis of nanostructured $NiFe_2O_4$ via a refluxing route, *Mater. Lett.*, 2008, **62** (12-13): 1973.

[20] Misra R.D.K., Gubbala S., Kale A., and Egelhoff Jr W.F., A comparison of the magnetic characteristics of nanocrystalline nickel, zinc, and manganese ferrites synthesized by reverse micelle technique, *Mater. Sci. Eng. B*, 2004, **111** (2-3): 164.

[21] Krehula S., Musić S., Skoko Z., and Popović S., The influence of Zn-dopant on the precipitation of α-FeOOH in highly alkaline media, *J. Alloys Compd*., 2006, **420** (1-2): 260.

[22] Inoue K., Okui M., Tanaka M., Shinoda K., Suzuki S., and Waseda Y., Influence of manganese on iron oxyhydroxides and oxides formed in aqueous solution, *Corros. Sci*., 2008, **50** (3): 811.

[23] Che A.X. and Li C.Z., Study on the preparation of homogeneous spindle-type a-FeOOH, *Chem. World*, 1997, **4**: 404.

[24] Kodama R.H., Berkowitz A.E., McNiff E.J., and Foner S. Surface spin disorder in $NiFe_2O_4$ nanoparticles. *Phys. Rev. Lett*., 1996, **77** (2): 394.

[25] Rezlescu L., Rezlescu E., Popa P.D., and Rezlescu N., Fine barium hexaferrite powder prepared by the crystallisation of glass, *J. Magn. Magn. Mater*., 1999, **193** (1-3): 288.

[26] Li D., Herricks T., and Xia Y., Magnetic nanofibers of nickel ferrite prepared by electrospinning, *Appl. Phys. Lett*., 2003, **83** (22): 4586.

[27] Carpenter E.E., O'Connor C.J., and Harris V.G., Atomic structure and magnetic properties of $MnFe_2O_4$ nanoparticles produced by reverse micelle synthesis, *J. Appl. Phys.*, 1999, **85** (8): 5175.